JOURNAL OF COMPUTATIONAL PHYSICS 26, 139–152 (1978)

A Simulation Model for Studying Low-Frequency Microinstabilities

W. W. LEE AND H. OKUDA

Plasma Physics Laboratory, Princeton University, Princeton, New Jersey 08540

Received March 11, 1976; revised July 30, 1976

A $2\frac{1}{2}$-dimensional, electrostatic particle code in a slab geometry has been developed to study low-frequency oscillations such as drift wave and trapped particle instabilities in a nonuniform bounded plasma. A drift approximation for the electron transverse motion is made which eliminates the high-frequency oscillations at the electron gyrofrequency and its multiples. It is, therefore, possible to study the nonlinear effects such as the anomalous transport of plasmas within a reasonable computing time using a real mass ratio. Several examples are given to check the validity and usefulness of the model, including those using full electron dynamics.

1. INTRODUCTION

Particle code simulation has become a well-established branch of plasma physics during recent years and is making crucial contributions to the understanding of the nonlinear processes inherent in plasma dynamics. Because of its flexibility, particle code simulation is quite useful and can be adopted easily for almost any kind of problem. Nonlinear behavior of microinstabilities of various origins, plasma heatings due to parametric processes and plasma diffusion caused by the low-frequency convective cells are a few of the examples in which the particle code simulation has played a central role.

While it is true that the particle code simulation is quite useful and flexible, most of the simulations have been carried out in an idealized geometry with unrealistic simulation parameters. For example, the periodic boundary conditions have generally been adopted to simulate an infinite homogeneous plasma. In addition, smaller mass ratios have also been used to squeeze the differences in frequencies associated with the motions of the electrons and ions so as to save the computing time.

In this paper we will describe a $2\frac{1}{2}$-dimensional simulation model which is useful for studying low-frequency waves produced by the spatial inhomogeneity in a bounded (finite) plasma. We will also show that reasonably realistic simulations can be carried out with the real mass ratio of the ions and the electrons by using the drift approximation for the electron transverse motion. We believe this is an important step in the direction of simulating a real fusion device such as a tokamak or a stellarator where the important processes are associated with the low-frequency fluctuations.

In Section 2, the model, including the dispersion character, the particle-pushing schemes, and the boundary conditions, is described. In Section 3, test results for the

0021-9991/78/0262-0139$02.00/0

model under various conditions using both full electron dynamics and guiding-center electrons are shown. Concluding remarks are given in Section 4 with a possible extension of the work.

2. Description of the Model

A. *Dispersion Relations*

In order to understand the basic properties of the $2\frac{1}{2}$-dimensional slab model, let us first derive the dispersion relation using the fluid approximation. We assume a configuration, shown in Fig. 1, where a uniform magnetic field $\mathbf{B}_0$ is in the z direction, a wavevector $\mathbf{k}$ is in the y–z plane, and θ is the angle between $\mathbf{B}_0$ and $\mathbf{k}$.

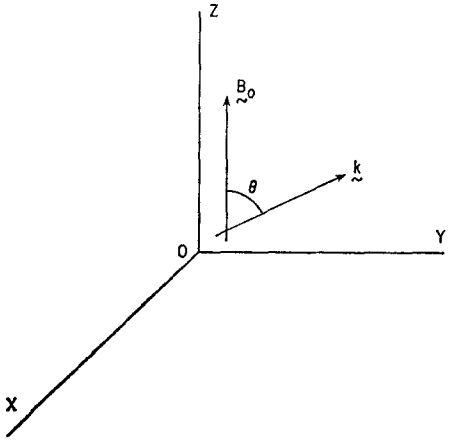

Fig. 1. Sketch of the configuration.

Following Braginskii [1], a set of two fluid equations can be written for a plasma as

$$\frac{\partial n_j}{\partial t} + \nabla \cdot (n_j \mathbf{v}_j) = 0,$$

$$\frac{\partial \mathbf{v}_j}{\partial t} + (\mathbf{v}_j \cdot \nabla)\, \mathbf{v}_j = \frac{e_j}{m_j}\left(\mathbf{E} + \frac{1}{c}\mathbf{v}_j \times \mathbf{B}_0\right), \tag{1}$$

$$\nabla^2 \phi = -4\pi e(n_i - n_e),$$

$$\mathbf{E} = -\nabla \phi,$$

$$j = \text{e and i},$$

where the thermal effects are neglected.

Linearizing Eq. (1) and assuming the perturbation quantities of the form $\exp(i\mathbf{k}\cdot\mathbf{x} - i\omega t)$, one obtains the simple dielectric function

$$\epsilon(k_\perp, k_\parallel, \omega) = 1 + \frac{\omega_{pi}^2}{\Omega_i^2 - \omega^2}\frac{k_\perp^2}{k^2} + \frac{\omega_{pe}^2}{\Omega_e^2 - \omega^2}\frac{k_\perp^2}{k^2} - \frac{k_\parallel^2}{k^2}\frac{\omega_{pi}^2}{\omega^2} - \frac{k_\parallel^2}{k^2}\frac{\omega_{pe}^2}{\omega^2}, \tag{2}$$

where ω_{pe} and ω_{pi} are the plasma frequencies and Ω_e and Ω_i are the gyrofrequencies of the electrons and the ions.

The dispersion relation is obtained from $\epsilon = 0$ and a sketch is given in Fig. 2a. In general, there are three branches of oscillations for an arbitrary angle of propagation. For parallel propagation ($\theta = 0$), the electron plasma waves and the cyclotron waves at $\Omega_{e,i}$ are the resonant oscillations. For perpendicular propagation ($\theta = \pi/2$), upper hybrid $\omega_{UH} = (\omega_{pe}^2 + \Omega_e^2)^{1/2}$, lower hybrid $\omega_{LH} = \omega_{pi}/(1 + \omega_{pe}^2/\Omega_e^2)^{1/2}$ resonances and the convective cell mode at $\omega = 0$ [2] are the three modes. When the warm plasma effects are considered, there are more natural oscillations such as electron and ion Bernstein modes, ion acoustic waves, and drift waves in an inhomogeneous media.

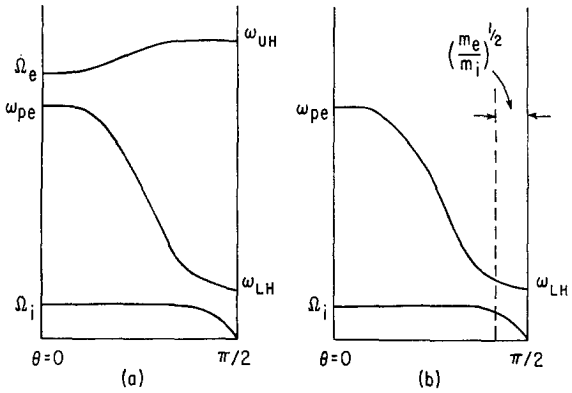

FIG. 2. Dispersion characteristics of the electrostatic waves in a magnetic field using full dynamics for electrons (a) and the guiding-center approximation for electrons (b).

Now let us consider what happens to the dispersion diagram if we make a drift approximation for the electron transverse motion across the magnetic field. Using $\mathbf{v}_\perp^e = c\mathbf{E}_\perp \times \mathbf{B}_0/B_0^2$ in Eq. (1), one finds

$$\epsilon(k_\perp, k_\parallel, \omega) = 1 + \frac{\omega_{pi}^2}{\Omega_i^2 - \omega^2}\frac{k_\perp^2}{k^2} - \frac{\omega_{pi}^2}{\omega^2}\frac{k_\parallel^2}{k^2} - \frac{\omega_{pe}^2}{\omega^2}\frac{k_\parallel^2}{k^2}. \tag{3}$$

Equation (3) can also be obtained by simply letting $\Omega_e \to \infty$ in Eq. (2). The corresponding dispersion diagram is shown in Fig. 2b. It is clear that there are no high-

frequency oscillations associated with the electron gyromotion in this case and at the same time all the low-frequency oscillations are unchanged. Since we are only interested in the problems with long-wavelength $k_\perp \rho_e < 1$, low-frequency $\omega < \omega_{pi}$, oscillations, where the electron transverse motion can be considered adiabatic, the use of this scheme will not alter the physics involved. On the other hand, the elimination of the high-frequency oscillations from the system lessens the restriction on the time step in the simulation.

Since various frequencies associated with the thermal fluctuations are naturally generated by the particle motion in the particle code simulation, it is important to determine the condition under which the fluctuations at $\omega \sim \Omega_e$ are negligible. The amplitude of the fluctuations near the electron gyrofrequency for $\Omega_e > \omega_{pe}$, which can be calculated by making use of the fluctuation–dissipation theorem for a plasma in thermal equilibrium, is given by [2]

$$\frac{E_k^2}{8\pi} = \frac{T_e}{2} \frac{\omega_{pe}^2 \sin^2 \theta}{\Omega_e^2 + \omega_{pe}^2 - 2\omega_{pe}^2 \cos^2 \theta} \tag{4}$$

for a mode **k**. As we can see, the fluctuations at the electron gyrofrequency are negligibly small for $\Omega_e^2 \gg \omega_{pe}^2$. Hence, this gives us one more limitation on the use of the electron guiding-center model in addition to the usual conditions of $k_\perp \rho_e < 1$ and $\omega \ll \Omega_e$.

The low-frequency oscillations of lower hybrid and drift waves that propagate nearly perpendicular to the magnetic fields ($k_\perp \gg k_\parallel$) are of the greatest interest to us. For such cases, the highest frequency of the system is of the order of the lower hybrid frequency $\omega_{LH} \cong \omega_{pi}$, which is usually much smaller than ω_{pe} or Ω_e. Therefore, large time steps can be taken in the code to reduce the computing time. It is also possible to carry this further by using the drift approximation for the ions as well. Schemes can even be developed to preserve the finite gyroradius effects. However, we will not consider such a case here. By keeping the full dynamics for the ions, the code is general enough to include the ion inertia and dissipative effects which are crucial for the stability of low-frequency microinstabilities [3].

B. *Particle Pushing Algorithm*

Let us now consider a $2\frac{1}{2}$-dimensional (five-dimensional phase space) slab model shown in Fig. 3. Since we are most interested in the modes propagating nearly perpendicular to the magnetic fields as described in the previous section, $\mathbf{B}_0(x)$ is oriented nearly along the z direction in our model with only a small component in y, i.e., $B_{0z} \gg B_{0y}$, $B_{0x} = 0$.

As we can see, the highest frequency in this configuration is of the order of ω_{pi}. Therefore, one would like to use a time step of

$$\omega_{pi} \Delta t \cong 0.25 \sim 0.5. \tag{5}$$

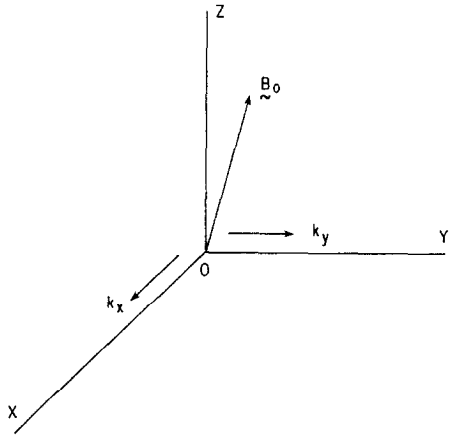

FIG. 3. Sketch of the simulation model.

One possible source of error in using such a large Δt may come from the free streaming of the electrons along the magnetic field lines. For cases of $k_\perp \gg k_\parallel$, the projection of the motion along the field lines into the x–y plane is quite small compared with the wavelength of the perturbation and therefore the particles will always experience a constant phase of the fluctuating field during one time step. Thus, the corresponding numerical error is negligible in the leap-frog scheme. However, significant errors may occur due to the transverse motion of the electrons for large Δt's when the amplitude of the fluctuating field is also large. The average displacement of the electrons across the magentic field for one Δt may be given by

$$\begin{aligned} \langle(\Delta x_e)^2\rangle^{1/2} &= \left\langle c^2 \frac{E_y^2}{B_0^2} \right\rangle^{1/2} \Delta t \\ &\approx \frac{\omega_{pe}}{\Omega_e} \left\langle \frac{E_y^2}{nT_e} \right\rangle^{1/2} v_e \, \Delta t, \end{aligned} \tag{6}$$

where v_e is the electron thermal speed, and E_y^2/nT_e is the field energy compared with thermal energy, which may be as large as 10^{-2} for strong instabilities. Since $\langle(\Delta x_e)^2\rangle^{1/2}$ must be much less than the wavelength of interest the restriction on Δt from Eq. (6) may be more severe than Eq. (5) unless Ω_e is much greater than ω_{pe}.

For the ion mover, the standard leap-frog scheme has been used [4]:

$$\frac{\mathbf{v}^i(t + \Delta t) - \mathbf{v}^i(t)}{\Delta t} = \frac{e}{m_i} \left[\mathbf{E}(t + \Delta t/2) + \frac{1}{2} (\mathbf{v}^i(t + \Delta t) + \mathbf{v}^i(t)) \times \mathbf{B}_0 \right],$$

$$\frac{\mathbf{x}^i(t + 3\Delta t/2) - \mathbf{x}^i(t + \Delta t/2)}{\Delta t} = \mathbf{v}^i(t + \Delta t).$$

For the electron parallel motion along the field lines, the leap-frog scheme has again been adopted:

$$\frac{v_{\parallel}^{e}(t+\Delta t)-v_{\parallel}^{e}(t)}{\Delta t}=-\frac{e}{m_e}E_{\parallel}(t+\Delta t/2),$$

$$\frac{x_{\parallel}^{e}(t+3\Delta t/2)-x_{\parallel}^{e}(t+\Delta t/2)}{\Delta t}=v_{\parallel}^{e}(t+\Delta t).$$

For the electron perpendicular motion across the field lines, a predictor–corrector method [5],

$$\frac{\mathbf{x}_{\perp}^{e*}(t+3\Delta t/2)-\mathbf{x}_{\perp}^{e}(t-\Delta t/2)}{\Delta t}=\frac{2c}{B_0^2}\mathbf{E}_{\perp}(t+\Delta t/2)\times\mathbf{B}_0,$$

$$\mathbf{x}_{\perp}^{e}(t+3\Delta t/2)=x_{\perp}^{e}(t+\Delta t/2)+\frac{\Delta t}{2}\frac{c}{B_0^2}[\mathbf{E}_{\perp}(t+\Delta t/2)+\mathbf{E}_{\perp}^{*}(t+3\Delta t/2)]\times\mathbf{B}_0,$$

has been used where $E_{\perp}^{*}(t+3\Delta t/2)$ is the predicted electric field obtained from the predicted particle location $x_{\perp}^{e*}$. As will be shown later, the scheme described above is accurate enough for the simulation of low-frequency drift wave instabilities for the time step of $\omega_{pi}\,\Delta t \approx 0.5$.

C. *Boundary Conditions*

The boundary conditions in plasma simulations using particle codes are rather sophisticated and have not been studied extensively in the past. This is because the effects of the boundaries interfere and modify the physics that one is trying to simulate. Since the size of the simulation plasma is usually small compared with the real one, these interferences can become very significant. This leads to the use of the periodic boundary conditions in most of the simulations, which enables one to deal with an infinite system free from boundaries. However, when a bounded (finite) plasma is used to simulate a nonuniform plasma, the boundary effects become unavoidable. Therefore, special care has to be taken in treating the plasma–boundary interactions to minimize the undesirable and unphysical effects. It is worth mentioning here that boundary effects are usually neglected in most of the theoretical analyses.

For the sake of definiteness, we consider an idealized system, as shown in Fig. 4. The plasma is nonuniform in x with a prescribed density profile $N(x)$ and is bounded by the conducting walls at $x = 0$ and L where the electrostatic potentials are zero. In the y direction, the plasma is uniform and is assumed periodic so that the waves can propagate through the system. In the following paragraphs, we will discuss different schemes that have been studied using this system. In order to make our discussions general enough for any bounded system, finite gyroradii for both electrons and ions are kept in the examples given below.

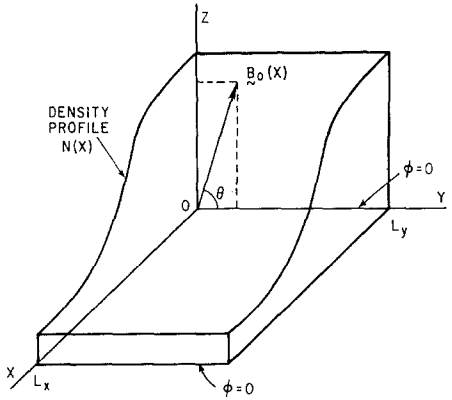

FIG. 4. Sketch of the nonuniform, bounded plasma model in a magnetic field.

It is obvious that the periodic condition in x is not appropriate here since the plasma is nonuniform in this direction. One might suggest that it would be possible to have periodicity in x by using a periodic density profile $N(x)$. Such a system is, of course, possible and we indeed tried it for the drift wave turbulence. However, a strong interference of two distinct drift waves excited at $dN/dx > 0$ and $dN/dx < 0$ regions was observed. This interference modified not only the linear phase of the instability but also its development in the nonlinear turbulent stage. Even if these two branches of the instability could be separated *in some way,* it is redundant to simulate two identical processes at the same time.

Let us now look at the usual reflecting boundary conditions where the out-of-bounds particles are reflected back to the original system at every time step with $x \to -x$ (or $x \to 2L - x$), and $v_x \to -v_x$. The immediate consequence of this scheme was the shift of the guiding-center positions of these particles both in the x and y directions. While the shift in y produced the usual sheath currents along the wall, the shift in x created regions with sharp density rgadients near the boundaries, the widths of which were of the order of several gyroradii. Due to the differences in gyroradii between electrons and ions, large sheath electric fields were also set up near the walls which, in turn, drove a strong $\mathbf{E} \times \mathbf{B}$ drift. The combined effects caused cross-current instabilities which seemed to be of the two stream or lower hybrid types. These instabilities are usually strong enough to completely mask the weak drift wave instabilities in the main body of the plasma. They are, of course, undesirable. In principle, the guiding-center shift in x can be eliminated by using a rather complicated and time-consuming scheme in which particles are reflected exactly at the boundary. Besides being impractical, this scheme still leaves us the sheath currents to reckon with.

Another obvious way to tackle the boundary problems is to use the absorbing wall condition, where all the particles reaching the boundaries are removed from the system. Again, regions with sharp density gradients appeared, and, because of the differences in gyroradii between the electrons and the ions, large electric fields were

also set up near the walls. The combined effects again caused the plasma to become unstable. To remedy this situation, one can emit particles back to the system. However, we found that the noise introduced by this scheme, due either to discrete particle effects or sheath formation, became intolerable when the time scale of the simulation was too long. Moreover, it is rather difficult to maintain a prescribed density profile near the wall with this method.

As we can see, the noise produced by the plasma–boundary interactions mainly comes from the disturbance of the guiding-center positions of the particles near the wall. It is further enhanced by the discreteness and smallness of the simulation plasma, and by the large number of time steps involved in the low-frequency simulations.

The method we finally settled upon is a combination of the absorption and reflection boundary conditions. In this scheme, particles are allowed to move freely in and out of the boundaries, mainly through gyrations. While outside, the particles are under the influence of a symmetric force field with respect to the wall and are advanced in time by the regular particle-pushing schemes, as are the particles inside. However, at every time step the positions of the out-of-bounds particles are temporarily mirror reflected back to the system for the purpose of charge distribution and diagnostic calculations. By doing so, we in fact assume that those particles never leave the system and, instead, traverse a trajectory, shown in Fig. 5. As we can see, the particles are

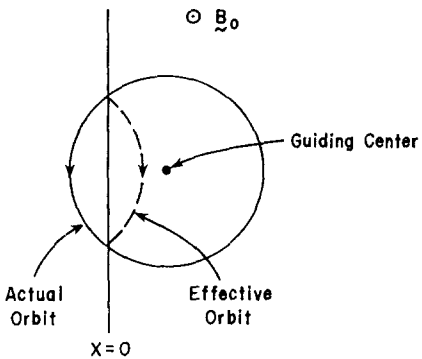

FIG. 5. Particle orbit near the boundary wall.

"reflected" exactly at the wall and the guiding centers are not disturbed in either direction in the process. Thus, the pitfalls mentioned earlier are eliminated and the prescribed density profiles near the wall maintained. Furthermore, the total charge and energy of the system are also conserved at each time step with this scheme. The change in the direction of gyration for the out-of-bounds particles shown in Fig. 5 should not present any problem to the bulk plasma if the system size is much larger than the gyroradius and the out-of-bounds particles do not drift too far from the system. These conditions are usually true for simulations. Since the potentials are set to zero at the wall, the drift in x for the particles due to E_y near the wall is always small. However, it is necessary to smooth out the potential fluctuations in y

completely near the wall in order to suppress associated noises. Without this smoothing scheme a weak numerical instability near the wall has been observed.

Satisfactory results have been obtained in using the treatment of the boundary particles mentioned above for the model shown in Fig. 4 to study drift wave instabilities. The noise due to the plasma–boundary interactions was small when the finite gyroradii were kept for both electrons and ions. With the guiding-center approximation for the electrons, noise from the wall was further reduced. This is because the electrons do not cross the boundaries associated with the gyromotion and are reflected by the scheme of $x \to -x$, $v_x \to -v_x$.

So far we have described the basic algorithm of the model useful for studying the low-frequency drift wave instabilities. Further modifications are necessary to study more complicated phenomena, such as the trapped particle instabilities where the trapping due to magnetic mirrors and the Coulomb collisions become essential. Such a model has been constructed and is being used to study the turbulent diffusion associated with the trapped particle instabilities [6]. We should point out here that this model may not be readily adaptable to electromagnetic codes becuase of the counterrotating particles involved.

3. Results of Simulations

A. *Test of the Boundary Conditions*

Let us first point out several important aspects of the particle code simulation for the low-frequency microinstabilities. As we know, the amplitude of the low-frequency fluctuations is quite small compared with that of the high-frequency oscillations at the lower hybrid resonance, due to the fact that low-frequency phenomena are always in the quasi-neutral state. Therefore, the energy conservation of the code has to be better than that of the high-frequency oscillations. Moreover, it is also important to keep the high-frequency electric field fluctuations of the simulation plasma low, because the low-frequency waves can easily be masked by the small amount of the high-frequency noises. In some cases, excessive noise of this kind in the system can completely suppress the coherent signals of the charge buildup associated with the microinstabilities. Since the growth time of the instability is usually long for a typical run compared with the allowable time step Δt, it makes these problems even more difficult to deal with.

With those in mind, we have first carried out the test of the bounded plasma model with the absorption–reflection boundary conditions for the case of a homogeneous plasma. The parameters of the run were: 64×32 grid, 256×64 particles for each species, a (particle size) $= 1.53$, $T_e/T_i = 4$, $m_i/m_e = 25$, $\Omega_e/\omega_{pe} = 2$, $\lambda_{De} = 2$, $\omega_{pe}\,\Delta t = 0.5$, and $\theta = 88.5°$. The units of the simulations are $\omega_{pe} = 1$, Δ(grid size) $= 1$. Figure 6 shows the time-averaged spectrum of the fluctuation field energy. Note that this run was made without the use of the guiding-center approximation for the electrons where the noise from the walls should be more pronounced.

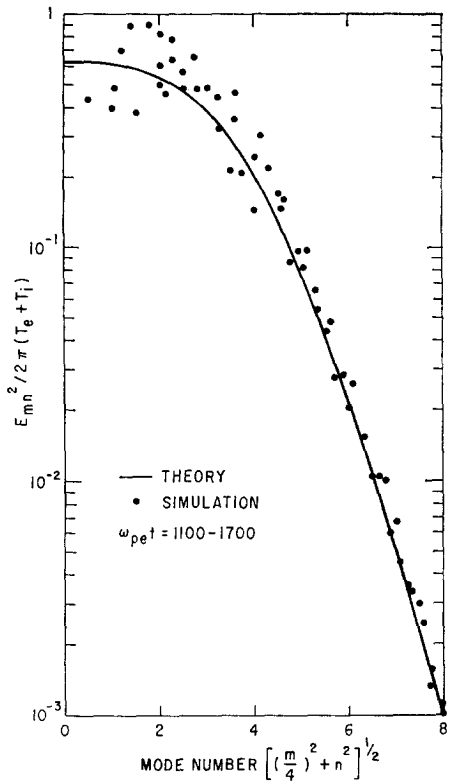

FIG. 6. Fluctuation spectrum for the bounded plasma model. The theoretical values are given by $E_k^2/8\pi = (1/T_e + 1/T_i)^{-1}/[1 + k^2\lambda_D^2 \exp(k^2a^2)]$.

As we can see, the agreement between the theoretical predictions and the numerical results is quite satisfactory. The noise excited near the boundaries was apparently small. The accumulated error for the total energy conservation of the system was about 0.2 %. For cases with other boundary conditions the plasma was much noisier and the conservation of energy was also worse. Wall-induced instabilities were also observed.

B. *Simulation of Drift Wave Instabilities*

Here we will present a few examples of the simulations in an inhomogeneous, bounded plasma, where the drift wave instability is dominated by one unstable mode.

The first example is the case in which we used the same particle-pushing schemes, i.e., schemes for full electron dynamics, and the same parameters as those in the previous run except for the density distribution where a hyperbolic tangent profile in x,

$$N(x) = N_0[1 - \kappa_0 l_0 \tanh(x - x_0)/l_0],$$

was used where $\kappa_0 = 0.1$, $l_0 = 24/\pi$, $x_0 = 32$, and N_0 was average number density. Figure 7 shows the growth of the electric field fluctuations for the most unstable mode and the spatially averaged density modulations in the homogeneous y direction. The growth rate agrees well with the theory taking into account the mode structure in the inhomogeneous x direction [7]. The error for the total energy conservation was about 0.2 % and no serious noises were created near the boundary.

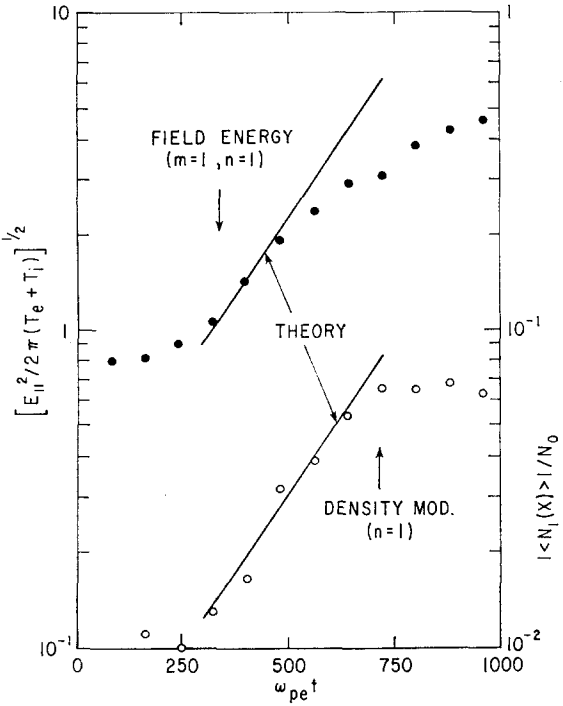

FIG. 7. Growth of the electric field and density fluctuations associated with the drift wave instability. The mass ratio is $m_i/m_e = 25$.

The second case is the example using a 64 × 64 grid with 256 × 128 particles for each species, $m_i/m_e = 100$, $T_e/T_i = 4$, $\lambda_{De} = 2$, $\Omega_e/\omega_{pe} = 4$, and $\theta = 88.6°$. Here the guiding-center model with $\omega_{pe}\,\Delta t = 4$ was used. The parameters for the density profile were $\kappa_0 = 0.07$, $x_0 = 32$, $l_0 = 34/\pi$. The linear phase of the instability is shown in Fig. 8, which also closely follows the theoretical prediction [7]. The total energy conservation was quite satisfactory and the error was less than 0.1 %.

The last example is the case using a *real* mass ratio $m_i/m_e = 1837$ on the 64 × 64 grid with the same number of particles, $\kappa_0 = 0.09$, $l_0 = 34/\pi$, $x_0 = 32$, $T_e/T_i = 9$, $\lambda_{De} = 2$, and $\theta = 89.1°$. To avoid the large step size of the $c\mathbf{E} \times \mathbf{B}_0/\mathbf{B}_0^2$ electron drift [Eq. (6)] in the guiding-center model, a strong magnetic field $\Omega_e/\omega_{pe} = 10$ and the time step $\omega_{pe}\,\Delta t = 10$ ($\Omega_e\,\Delta t = 100$) were used. The growth of the electric

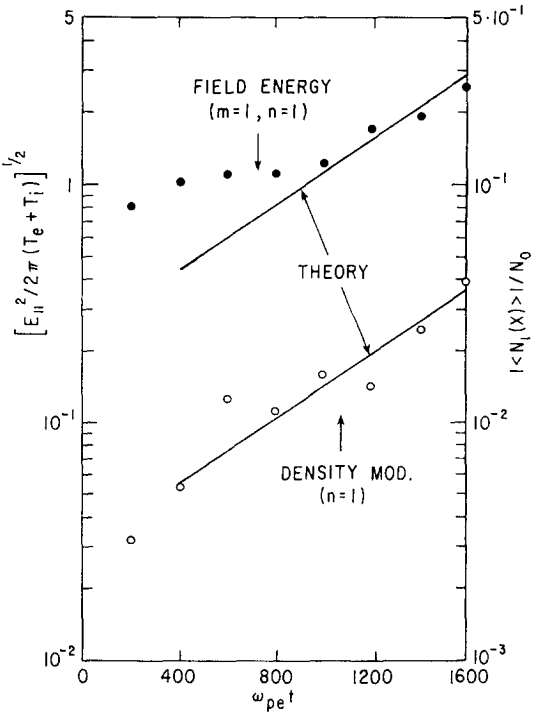

FIG. 8. Drift wave instability with mass ratio $m_i/m_e = 100$.

field energy is shown in Fig. 9 together with the development of the density modulation in the y direction. A strong instability developed again with the theoretically predicted linear growth rate [7]. The error for the total energy conservation was 0.1 % at the end of the run, where the instability had reached the saturation stage. The total running time (CPU) was approximately 2 hours on the IBM 360/91. This indicates that it is feasible to simulate low-frequency microinstabilities using real plasma parameters within a reasonable computing time with our model.

The details of the simulation results for the drift wave instabilities have been reported elsewhere [7, 8]. Let us describe briefly the significance of these results. First of all, we were able to provide detailed comparisons with the existing linear theories, hitherto unavailable from the laboratory experiemnts. The anomalous diffusion and conductivity coefficients were also calculated from the observed particle and energy transport across the magnetic field in the inhomogeneous direction. These scaling laws are important, for example, for the numerical modeling of the tokamak transport. Furthermore, we were also able to shed some light on the most important and, yet, unresolved question concerning the nonlinear evolution of the instability. The results indicated that the quasi-linear decay of the density profile was responsible for the nonlinear saturation, and the energy transport was mainly the result of the density profile change which, in turn, altered the local dispersions. With these

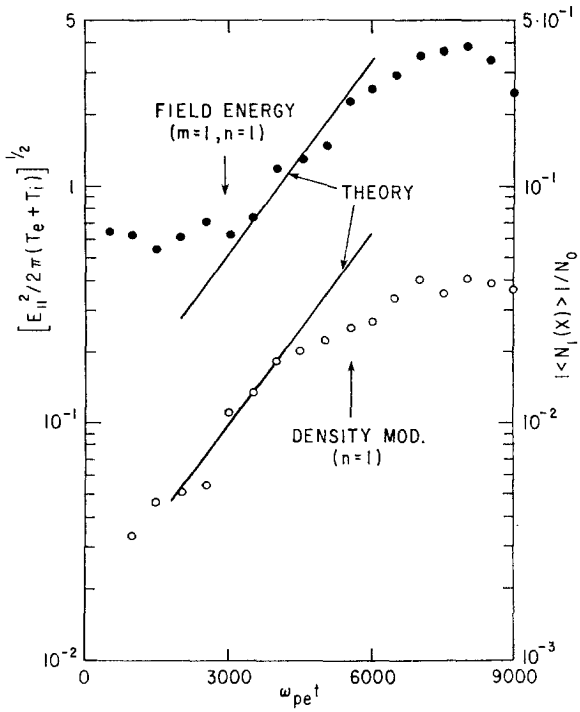

FIG. 9. Drift wave instability with the real mass ratio $m_i/m_e = 1837$.

observations, a self-consistent quasi-linear theory has been developed [8]. Very good agreement was found between the theory and the simulation in the time evolution of the instability. This shows the importance of the particle code simulation for studying low-frequency microinstabilities where the kinetic effects such as Landau damping and finite gyroradius are of fundamental importance.

Let us make one brief comment on the usefulness of the quiet start technique for suppressing the random noises in drift wave simulations. We have tried the technique by loading the phase space uniformly with the weighted charge and mass for each particle in the inhomogeneous x direction according to a prescribed density profile. Unfortunately, however, the numerically induced beam instability associated with the quiet start scheme, which was in the form of the loss cone instability for a magnetized plasma, modified the drift instability substantially at the later stage of the development. This is because, under the normal circumstances for the simulation, the growth rate of the drift mode is comparable to that of the beam loss cone mode. The latter is usually a small fraction of the ion cyclotron frequency depending on the number of beams in the phase space. Therefore, additional smoothing of the ion orbit seems to be necessary in order to eliminate the beam loss cone mode. However, the smoothing in five-dimensional phase space appears prohibitive.

4. Concluding Remarks

We have developed a $2\frac{1}{2}$-dimensional particle code which can simulate nonuniform plasmas in a bounded system where the plasma–wall interactions are carefully eliminated. Using guiding-center drift approximation for the electron transverse motion, we have shown that it is possible to simulate real plasmas within a reasonable computing time using the presently available computers. The results obtained indicate good agreement with the existing linear theory in the case of collisionless drift waves.

It is also possible to extend the present model to a full three dimensions. The transverse drift motion should cause no difficulty. The longitudinal motion, on the other hand, may give us trouble when large time steps are employed. Since one is interested in the low-frequency microinstabilities such as those existing in a tokamak, it is possible to truncate the phase space such that only the modes $k_\perp \gg k_\parallel$ are kept, because those are the most dangerous oscillations. For such a case, again it is feasible to use a large time step Δt along the lines of force.

We have given examples only for the simulation of drift waves ($\omega < \Omega_i$). However, it should be emphasized that the model can be extended to include the polarization drift to study the high-frequency phonomena such as the lower hybrid heating, since the full dynamics are retained for moving the ions. For higher-frequency problems, the full dynamics for the electrons is then necessary.

As discussed in Ref. [4], it is also possible to use the exact particle mover with large $\omega_{ce}\,\Delta t$ (>1) in a uniform magnetic field without employing the guiding center formalism. However, the use of the guiding center formalism is necessary when dealing with the spatially varying magnetic fields such as those existing in a tokamak. Computer modeling of tokamaks is, of course, one of our aims.

Acknowledgments

The authors would like to thank Mr. R. F. Kluge for his assistance in computing. This work is supported by the U. S. Energy Research and Development Administration (formerly AEC) under Contract E (11-1)-3073.

References

1. S. I. Braginskii, *in* "Reviews of Plasma Physics" (M. A. Leontovich, Ed.), Vol. 1, 0. 214, Consultants Bureau, New York, 1965.
2. H. Okuda and J. M. Dawson, *Phys. Fluids* **16** (1973), 408.
3. R. R. Rukhadze and V. P. Silin, *Usp. Fiz. Nauk* **96** (1968), 87; *Soviet Physics Usp.* **11** (1969), 659.
4. O. Buneman, *J. Computational Phys.* **1** (1967), 517.
5. R. W. Hamming, "Introduction of Applied Numerical Analysis," p. 203, McGraw–Hill, New York, 1971.
6. Y. Matsuda and H. Okuda, *Phys. Rev. Lett.* **36** (1976), 474.
7. W. W. Lee and H. Okuda, *Phys. Rev. Lett.* **36** (1976), 870.
8. Y. Y. Kuo, W. W. Lee, and H. Okuda, in preparation.